

Coulomb-blockade oscillations in the conductance of a silicon metal-oxide-semiconductor field-effect-transistor point contact

C. de Graaf, J. Caro, and S. Radelaar

Delft Institute of Microelectronics and Submicron Technology, Delft University of Technology, Lorentzweg 1, 2628 CJ Delft, The Netherlands

V. Lauer and K. Heyers

Institute of Semiconductor Electronics, Aachen Technical University, D-5100 Aachen, Germany

(Received 19 February 1991; revised manuscript received 3 June 1991)

The low-temperature conductance of a point contact in a Si metal-oxide-semiconductor field-effect transistor shows periodic oscillations just above pinchoff. The experimental results on the oscillations quantitatively agree well with the model of the Coulomb blockade of resonant tunneling.

Recent experiments on one-dimensional silicon metal-oxide-semiconductor field-effect transistors^{1,2} (1D Si-MOSFET's) and 1D channels in GaAs devices^{3,4} just above threshold and at low temperatures revealed oscillations of the conductance *periodic* in gate voltage. Not only the periodicity distinguishes the periodic conductance oscillations (PCO) from universal conductance fluctuations (UCF), but also the fact that they are *absent* in the magnetoconductance.⁴ Two models have subsequently been proposed to explain the PCO: the Wigner crystal or charge-density-wave (CDW) model^{1,2} and the model of the Coulomb blockade (CB) of resonant tunneling.^{4,5,6} Common to both models is that a small segment is partially isolated in a narrow channel and that electron transport through the segment cannot be described by noninteracting electrons. The segment can be formed accidentally by two charged sites along the channel or intentionally by barriers defined using, for instance, a split-gate technique.^{7,8} The accidental charges or intentional barriers act either as pinning centers for a CDW or as tunnel barriers with resistance R_b (CB model). Oscillations in the conductance as a function of gate voltage then arise from sequential charging of the segment by one electron per oscillation. For a CDW, the conductance has a minimum if the segment length L_{segm} (the distance between the charges) equals an integral number of periods of the density wave, i.e., if the number of electrons in the segment is integral. In the CB model the oscillations are explained by the fact that the Coulomb interaction between electrons prevents an electron to tunnel into the segment, unless that electron has enough extra energy to overcome the charging energy $E_c = e^2/2C_t$. C_t is the total capacitance of the segment, including self-capacitance. If $E_c \gg \Delta E$ (ΔE is the level spacing in the segment) and if for both barriers $R_b > R_q = h/4e^2$ (the quantum resistance), then the conductance will be governed by the Coulomb blockade and will, upon changing gate voltage, oscillate with a period determined by the capacitance between segment and gate (Coulomb-blockade oscillations).

In this Brief Report we present experimental data on

periodic oscillations in the conductance of a Si-MOSFET point contact. Our data for these point contacts largely confirm those reported for long channels. Thus, also here the PCO must arise from transport through an isolated segment. This is striking in view of the short channel length of the point contact and the corresponding small number of charges available to delimit a segment. In addition, we found that the period of the oscillations periodic in the upper gate voltage (defined below) depends on the pinchoff voltage, i.e., on the electrical width of the point contact. We will show that our experimental results quantitatively agree well with the Coulomb-blockade model.

The devices used in the experiments are dual gate, n -channel Si-MOSFET's in which a point contact, i.e., a short and narrow constriction in the two-dimensional electron gas (2DEG), can be defined electrostatically. They are the MOSFET counterpart of the ballistic GaAs-Al_{1-x}Ga_xAs point contact which is well known for its quantized conductance as a function of width.⁹ The electrical properties of the MOSFET point contact, however, are completely different since the transport in the metallic regime is diffusive. We fabricated the point contacts on the same wafer as the multiple quantum wire devices described before.¹⁰ Figure 1 shows a schematic view of the device with the relevant layers. Both the lithographic width W_{lith} and length L_{lith} of the gap in the lower gate are about 100 nm. Outside this $100 \times 100 \text{ nm}^2$ area W_{lith} increases quickly. The mobility of the devices at 4.2 K, when a homogeneous 2DEG is formed by applying the appropriate gate voltage ratio, is $5 \times 10^3 \text{ cm}^2/\text{V s}$.

All measurements have been performed in a dilution refrigerator equipped with a superconducting magnet. We used a conventional ac lockin technique to determine the conductance of the point contacts as a function of upper gate voltage V_{GU} , lower gate voltage V_{GL} , and magnetic field B (oriented perpendicular to the 2DEG). The source-drain voltage V_{DS} was kept below kT/e . Measurements of the derivative dI_D/dV_{DS} of the drain current I_D as a function of V_{DS} were also performed.

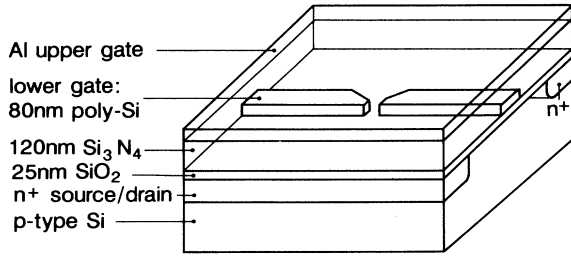


FIG. 1. Schematic drawing of the MOSFET point contact.

We measured the two terminal conductance G of fifteen point contacts as a function of V_{GU} (at constant V_{GL}) and V_{GL} (at constant V_{GU}). For constant V_{GU} above the threshold voltage $V_{GU,T}$ of the remote 2DEG leads, the G - V_{GL} curves have a kink at the threshold voltage $V_{GL,T}$ of the lower gate. Below $V_{GL,T}$ the point-contact is defined. Both types of point contact conductance traces have a clear pinchoff voltage $V_{GU,P} > V_{GU,T}$ and $V_{GL,P} < V_{GL,T}$, respectively, below which the point contact does not conduct. In an ideal point contact the bottom of the conduction band has a smooth saddle shape, the saddle point lying eV_0 above the bottom of the conduction band in the wide 2DEG leads. In a real device, however, potential variations are superimposed on the saddle shape due to randomly distributed charges in the gate oxide and at the Si-SiO₂ interface. For $V_{GU} > V_{GU,P}$ and $V_{GL,P} < V_{GL,T}$ the Fermi energy E_F exceeds eV_0 , the point contact conducts and the electrical width $W < W_{\text{lith}}$ of the point contact is defined. W and eV_0 are influenced by both gate voltages, while only V_{GU} determines E_F .

In the conductance traces two transport regimes can be distinguished. If we combine V_{GU} and V_{GL} in such a way that $E_F \gg eV_0$, the point contact operates in the metallic regime and the conductance shows UCF (Ref. 11) and plateaulike features¹¹ reminiscent of the quantized conductance of ballistic point contacts. The second regime is defined by $E_F \approx eV_0$, where the point contact is close to pinchoff. Here the influence of the potential variations on G is of the same order as G itself. Indeed in this strongly localized regime all measured point contacts have large reproducible conductance peaks of magnitude $G_{\text{max}} \lesssim 0.5e^2/h$. For most of our devices these peaks are randomly spaced in gate voltage.

For two point contacts arranged in one MOSFET, however, we find periodic conductance oscillations just above pinchoff. This is shown in Fig. 2 for point contact PC2, to which we restrict ourselves since the results for PC1 are very comparable. The positions of the pronounced peaks in the Fourier spectra of the data [see the insets of Figs. 2(a) and 2(b)] give oscillation periods $\Delta V_{GL} = 9$ mV and $\Delta V_{GU} = 13$ mV. We studied the temperature dependence of the PCO in the G - V_{GU} traces in detail between 100 and 900 mK. In this range the amplitude of the PCO decreases gradually with increasing temperature. At 900 mK the oscillations were small, but still visible. Extrapolation to zero amplitude gives the temperature $T_0 = 1.1$ K at which the oscillations are completely

smearred. From the temperature dependence of fifteen successive oscillations we found that G is thermally activated in the oscillation minima with activation energy $E_{A,\text{min}} = 0.13 \pm 0.05$ meV. Also in the maxima G seems to follow an activated behavior, although with a much smaller activation energy $E_{A,\text{max}} = 15 \pm 6$ μ eV. For each temperature the full width at half maximum of the oscillations is equated to 3.5 kT. This gives the relation between V_{GU} and $E_F - eV_0$ in the leads directly outside the segment: $d(E_F - eV_0)/dV_{GU} = 31.4$ meV/V. Due to the decrease of eV_0 with V_{GU} , this value is much larger than $dE_F/dV_{GU} = 1.7$ meV/V in the 2DEG leads, indicating that the segment lies well inside the point contact. Between successive oscillations the increase of E_F outside the segment with respect to eV_0 is $\Delta(E_F - eV_0) = [d(E_F - eV_0)/dV_{GU}] \Delta V_{GU} = 0.41$ meV.

Figure 3 shows a selection of G - V_{GU} curves measured at various fields B . Here again the oscillations are roughly periodic, with a mean period that remains constant up to 10 T. By carefully comparing all measured $G(B)$ - V_{GU} curves, each individual oscillation can be traced from 0 to 10 T. The amplitude and background of the oscillations, however, depend strongly on B . These results qualitatively confirm those reported by Staring *et al.*⁴ We also measured G as a function of B at several V_{GU} . The overall behavior of a conductance peak was to

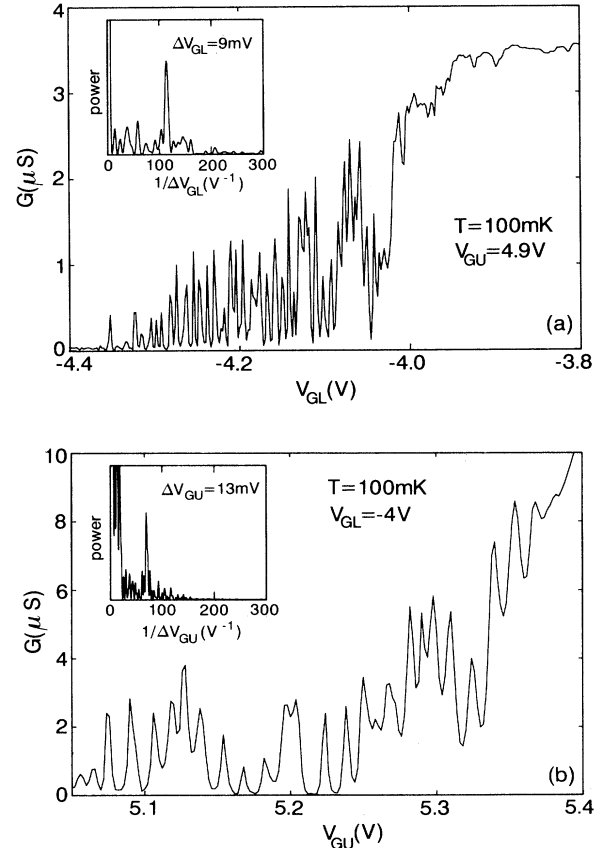


FIG. 2. Periodic conductance oscillations as a function of (a) V_{GL} and (b) V_{GU} at $T=0.1$ K and $B=0$. Insets: Fourier spectra of the data.

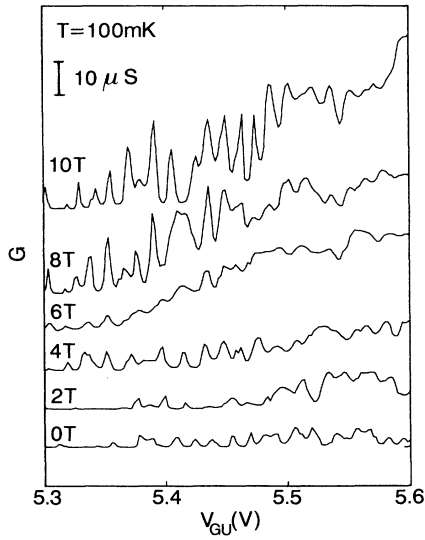


FIG. 3. Evolution of the PCO at $T=0.1$ K as B is increased from 0 to 10 T. $V_{GL} = -4.0$ V. The curves are offset for clarity.

increase with B , while G in the minima reached a maximum between 5 and 7 T, but decreased again for higher fields. This makes the PCO hardly observable around 6 T (see Fig. 3).

The data presented so far were obtained with small V_{DS} , so that I_D was proportional to V_{DS} . At higher V_{DS} , however, the I_D - V_{DS} characteristic was highly nonlinear. Figure 4 shows this effect in the differential conductance dI_D/dV_{DS} near a maximum and a minimum of the PCO. A threshold for conduction ($V_T \approx 0.2$ mV) and an overshoot in dI_D/dV_{DS} are characteristic for a minimum. The asymptotic slope of the I_D - V_{DS} curves yields the approximate point-contact resistance $R_p \approx 100$ k Ω in the gate voltage regime where PCO occur.

We found that $V_{GU,P}$ changes randomly with time. The period ΔV_{GU} , on the other hand, shows a clear trend to increase with increasing $V_{GU,P}$ (see Fig. 5). To explain

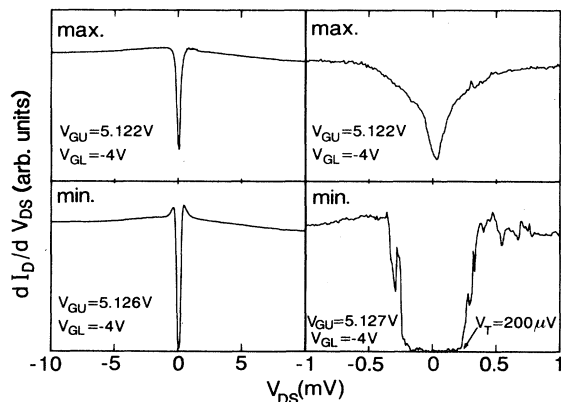


FIG. 4. Left: dI_D/dV_{DS} vs V_{DS} near a conductance maximum and minimum at $T=100$ mK. Right: expanded plots exactly in the maximum and minimum.

this effect we first discuss the charges forming the isolated segment. An estimate¹² for the width W of the point contact is 30 nm. Then, the estimated length L of the point contact is $L = L_{\text{lith}} + 2(W_{\text{lith}} - W)/2 \approx 170$ nm. The densities of fixed oxide charge and interface traps, derived from C - V measurements on MOS capacitors from the device wafer, are $N_f \approx 1.7 \times 10^{11}$ cm⁻² and $D_{it} \approx 8 \times 10^{10}$ cm⁻²eV⁻¹ (midgap). Fixed charges are positive,¹³ whereas for a MOS structure biased in inversion the number of neutral and negative interface traps is approximately equal.¹³ Thus, statistically, for a uniform D_{it} the estimated number of charges in the point contact is 11. Taking into account the U shape of D_{it} this number will be several times higher and in principle high enough to isolate a segment. From our experimental observation, however, that only two out of 15 point contacts show PCO we conclude that only a fraction of the charges is effective in delimiting an isolated segment. Both in the CB model and the CDW model the oscillation period depends on L_{segm} . A change of L_{segm} (i.e., formation of a new set of tunnel barriers or pinning centers) can occur due to trapping or detrapping of charges. This could lead to a change in $V_{GU,P}$, but such changes would not necessarily correlate with changes of L_{segm} . Also, for the very short channel in our device it is likely that occasionally no pair of tunnel barriers or pinning centers would be available, which is contrary to our observation that the PCO never disappeared (as long as the device was not warmed up to room temperature). Consequently, L_{segm} must be constant. In our opinion a change of $V_{GU,P}$ is due to an overall change of trapped charge close to the point contact, which has an effect similar to a change of V_{GL} . Other measurements (not on PC1 or PC2) show that a more negative V_{GL} gives a higher $V_{GU,P}$ and a less steep G - V_{GU} curve, i.e., higher eV_0 and stronger confinement (approximately 5% width decrease per volt increase of $V_{GU,P}$). Figure 5 can now be understood qualitatively from $\Delta V_{GU} \propto (WL_{\text{segm}})^{-1}$. For the CB model this follows from $\Delta V_{GU} \propto C_{GU}^{-1}$, while for the CDW model this follows from the property that an oscillation minimum occurs if an integral number of periods

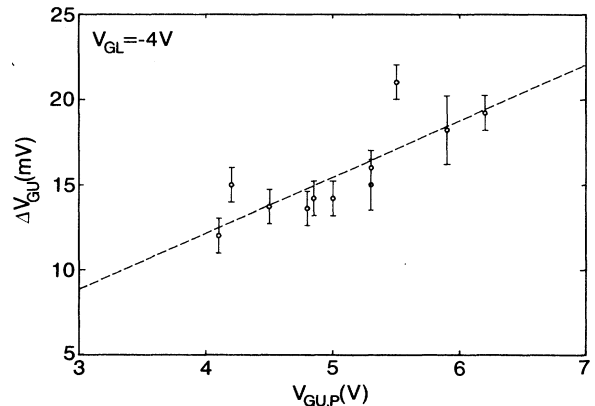


FIG. 5. Period ΔV_{GU} of the conductance oscillations vs pinchoff voltage $V_{GU,P}$ at $V_{GL} = -4$ V. The dashed line is a linear fit to the data.

of the wave fits in the segment.

We now proceed with the quantitative analysis of the experimental results. Our data $2E_{A,\min}=0.26\pm 0.1$ meV, $2eV_T\approx 0.4$ meV, $\Delta(E_F - eV_0)\approx 0.41$ meV, and $3.5kT_0\approx 0.33$ meV are approximately equal. The Coulomb-blockade model applied to our point contacts indeed predicts^{6,14} the following relation between the charging energy and the measured quantities: $2E_c=2E_{A,\min}=2eV_T=\Delta(E_F - eV_0)\approx 3.5kT_0$. The high point-contact resistance $R_p\gg h/4e^2$ also suggests Coulomb-blockade-induced conductance oscillations. Thus, in the remainder of this paper we will speak in terms of the Coulomb-blockade model.

Using $2E_c=e^2/C_t=0.35$ meV we find the total segment capacitance $C_t=4.5\times 10^{-16}$ F. An estimate for the level spacing ΔE in the segment, using $L\approx 170$ nm as the length of an infinitely high square-well potential, is $50\ \mu\text{eV}$. As the barriers of the segment are much less hard than this, we have $\Delta E\ll 50\ \mu\text{eV}$. Consequently, the ‘‘classical’’ Coulomb-blockade regime, where $E_c\gg\Delta E$, applies here. The capacitance formula $\Delta Q=e=C_{UG(LG)}\Delta V_{UG(LG)}$ gives the capacitances $C_{GU}=1.2\times 10^{-17}$ F and $C_{GL}=1.8\times 10^{-17}$ F between the segment and the upper and lower gate, respectively. From the parallel plate capacitor formula, C_{GU} and the insulator thickness¹⁰ we can calculate an area $A\approx 4.2\times 10^4$ nm². This area is much too large for an isolated segment situated in the nearly pinched off point contact. However, the parallel plate capacitance is greatly enhanced above $\epsilon A/t$ when the insulator thickness $t\geq\sqrt{A}$ and when other conductors are close. So, A will be much smaller.

The fact that the period of the PCO does not depend on B up to 10 T agrees with the CB model, under the condition that $\Delta E(B)\ll e^2/C_t$ holds in this magnetic-field range. Amplitude and background of the oscillations are determined by the tunnel rates through the barriers forming the isolated segment and by boundary scattering. Usually, both are highly influenced by a magnetic field. Inclusion of these effects in the CB model may possibly explain the observed large amplitude and

background variations as a function of B .

Changing V_{DS} is an alternative way to sweep E_F along the levels in the isolated segment. The CB model predicts a threshold V_T and steps in the I_D - V_{DS} characteristic. The abruptness of the steps in the ‘‘Coulomb staircase’’ depends on the dissimilarity of the two barriers.¹⁴ For equal barriers the steps are completely smoothed. But, by iterating the semiclassical master equation,¹⁴ we found that even in the case of equal barriers at $T\approx 100$ mK the first few ‘‘steps’’ should be observable as small peaks in dI_D/dV_{DS} . Numerical simulations,¹⁵ however, show that in low-dimensional systems the energy relaxation rate of electrons is reduced. So, a possible reason why we do not observe the small peaks is heating of electrons in the segment high above 100 mK.¹⁶ But, our measured dI_D/dV_{DS} curves for the minima are very similar to curves measured below the pinchoff voltage of point contacts not showing PCO. In that case only one, electrostatically induced, barrier is active. From this we conclude that bias-induced weakness of one of the barriers prevents observation of the Coulomb staircase.

In conclusion, we observed periodic oscillations in the conductance of a Si-MOSFET point-contact device. We analyzed the experimental data in the framework of the Coulomb-blockade model, and found good agreement between experiment and theory. In addition, we showed that the observed oscillation period variations are due to a change of the segment width and not to a change of the segment length. The magnetic-field dependence of the oscillation amplitude and the background of the conductance traces remains to be clarified.

We thank P. Balk, D. Laschet, M. Offenbergh, A. H. Verbruggen, and L. E. M. de Groot for their contributions to device realization and C. W. J. Beenakker, H. M. Jäger, C. J. P. M. Harmans, H. M. A. Schleijsen, and A. A. M. Staring for useful discussions. This work is part of the research program of the ‘‘Stichting voor Fundamenteel Onderzoek der Materie (FOM),’’ which is financially supported by the ‘‘Nederlandse Organisatie voor Wetenschappelijk Onderzoek (NWO).’’

¹J. H. F. Scott-Thomas, Stuart B. Field, M. A. Kastner, Henry I. Smith, and D. A. Antoniadis, Phys. Rev. Lett. **62**, 583 (1989).

²Stuart B. Field, M. A. Kastner, U. Meirav, J. H. F. Scott-Thomas, D. A. Antoniadis, H. I. Smith, and S. J. Wind, Phys. Rev. B **42**, 3523 (1990).

³U. Meirav, M. A. Kastner, M. Heiblum, and S. J. Wind, Phys. Rev. B **40**, 5871 (1989).

⁴A. A. M. Staring, H. van Houten, C. W. J. Beenakker, and C. T. Foxon, in *High Magnetic Fields in Semiconductor Physics III*, edited by G. Landwehr (Springer, Berlin, 1991).

⁵H. van Houten and C. W. J. Beenakker, Phys. Rev. Lett. **63**, 1893 (1989).

⁶C. W. J. Beenakker, Phys. Rev. B **44**, 1646 (1991).

⁷U. Meirav, M. A. Kastner, and S. J. Wind, Phys. Rev. Lett. **65**, 771 (1990).

⁸L. P. Kouwenhoven (private communication).

⁹B. J. van Wees *et al.*, Phys. Rev. Lett. **60**, 848 (1988); D. A.

Wharam *et al.*, J. Phys. C **21**, L209 (1988).

¹⁰J. R. Gao, C de Graaf, J. Caro, S. Radelaar, M. Offenbergh, V. Lauer, J. Singleton, T. J. B. M. Janssen, and J. A. A. J. Perenboom, Phys. Rev. B **41**, 12 315 (1990).

¹¹C. de Graaf (unpublished).

¹²Experiments on multiple-quantum-wire devices (Ref. 10), also with a 100-nm-wide gap in the lower gate, give $W=60$ nm in the metallic regime. In our case the confinement is stronger, leading to the estimate $W=30$ nm, which corresponds very well with W calculated by S. E. Laux and F. Stern, Appl. Phys. Lett. **49**, 91 (1986).

¹³E. H. Nicollian and J. R. Brews, *MOS Physics and Technology* (Wiley, New York, 1982).

¹⁴M. Amman, K. Mullen, and E. Ben-Jacob, J. Appl. Phys. **65**, 339 (1989).

¹⁵U. Bockelmann and G. Bastard, Phys. Rev. B **42**, 8947 (1990).

¹⁶D. V. Averin and A. N. Korotkov, Zh. Eksp. Teor. Fiz. **97**, 1661 (1990) [Sov. Phys. JETP **70**, 937 (1990)].